

# N domain of the Lon AAA+ protease controls assembly and substrate choice

Breann L. Brown,<sup>1</sup> Ellen F. Vieux,<sup>1,2</sup> Tejas Kalastavadi,<sup>1,2</sup> SaRa Kim,<sup>1,2</sup> James Z. Chen,<sup>1,2</sup> and Tania A. Baker<sup>1,2\*</sup>

<sup>1</sup>Department of Biology, Massachusetts Institute of Technology, Cambridge, Massachusetts

<sup>2</sup>Howard Hughes Medical Institute, Chevy Chase, Maryland

Received 3 August 2018; Accepted 12 November 2018

DOI: 10.1002/pro.3553

Published online 20 December 2018 proteinscience.org

**Abstract:** The protein quality control network (pQC) plays critical roles in maintaining protein and cellular homeostasis, especially during stress. Lon is a major pQC AAA+ protease, conserved from bacteria to human mitochondria. It is the principal enzyme that degrades most unfolded or damaged proteins. Degradation by Lon also controls cellular levels of several key regulatory proteins. Recently, our group determined that *Escherichia coli* Lon, previously thought to be an obligate homo-hexamer, also forms a dodecamer. This larger assembly has decreased ATPase activity and displays substrate-specific alterations in degradation compared with the hexamer. Here we experimentally probe the physical hexamer–hexamer interactions and the biological roles of the Lon dodecamer. Using structure prediction methods coupled with mutagenesis, we identified a key interface and specific residues within the Lon N domain that participates in an intermolecular coiled coil unique to the dodecamer. With this knowledge, we made a Lon variant (Lon<sup>VQ</sup>) that forms a dodecamer with increased stability, as determined by analytical ultracentrifugation and electron microscopy. Using this altered Lon, we characterize the Lon dodecamer's activities using a panel of substrates. Lon dodecamers are clearly functional, and complement critical *lon*- phenotypes but also exhibit altered substrate specificity. For example, the small heat shock proteins IbpA and IbpB are only efficiently degraded well by the hexamer. Thus, by elucidating the intermolecular contacts connecting the hexamers, we are starting to illuminate how

**Abbreviations:** AUC, analytical ultracentrifugation; EM, electron microscopy; Ibp, inclusion body binding protein; sHSP, small heat shock protein.

Additional Supporting Information may be found in the online version of this article.

**Summary statement** Lon protease degrades several critical regulatory proteins and maintains protein quality control. We characterized a variant of *Escherichia coli* Lon that preferentially forms a dodecamer; an assembly that has distinct activities and substrate recognition compared with the Lon hexamer. This variant served as a molecular probe to investigate the biological roles of the dodecamer–hexamer equilibrium *in vivo* and *in vitro*. This work thus highlights new aspects of the complex molecular processes that control Lon activity.

Tejas Kalastavadi's current address is Department of Studies in Genetics and Genomics, University of Mysore, Manasagangotri, Mysore 570006, India.

James Z. Chen's current address is Department of Biochemistry and Molecular Biology, Oregon Health and Science University, Portland, OR, USA.

The authors declare no competing interests.

Grant sponsor: Burroughs Wellcome Fund Postdoctoral Enrichment Program Fellowship 1015092; Grant sponsor: Division of Biological Infrastructure NSF-0070319; Grant sponsor: Jane Coffin Childs Memorial Fund for Medical Research 61-1529; Grant sponsor: Howard Hughes Medical Institute; Grant sponsor: National Institutes of Health F32GM094994.

\*Correspondence to: Tania A. Baker, Massachusetts Institute of Technology, 77 Massachusetts Ave, 68-523, Cambridge, MA 02139, USA. E-mail: tabaker@mit.edu

**dodecamer formation versus disassembly can alter Lon function under conditions where controlling specific activities and substrate preferences of this key protease may be advantageous.**

**Keywords:** AAA+ family; electron microscopy; crosslinking; analytical ultracentrifugation; coiled coils; regulated proteolysis

## Introduction

The protein quality control (pQC) network is integral for maintaining cellular homeostasis and viability during and after stress by preventing the accumulation of potentially toxic unfolded, damaged, and aggregated proteins. This system is composed of several enzymatic machines, including protein chaperones, disaggregases, and proteases. One of the central proteases responsible for pQC is Lon, as it degrades the majority of unfolded proteins in bacteria and is thought to perform a similar function in human mitochondria.<sup>1,2</sup> Lon is a highly conserved member of the AAA+ (ATPases associated with diverse cellular activities) protease family, which also includes ClpAP, ClpXP, FtsH, HslUV, and the 26S proteasome.<sup>3</sup> In bacteria, Lon also modulates levels of several short-lived regulatory proteins induced during cellular stresses, including heat shock and DNA damage.<sup>4-6</sup> In humans, mitochondrial Lon antagonizes aging by degrading oxidatively damaged proteins,<sup>7</sup> and Lon is identified as a potential therapeutic target to treat both lymphoma and bladder cancer.<sup>8,9</sup>

Lon assembles into a barrel-shaped homo-hexamer with the proteolytic active sites sequestered in an internal chamber, largely inaccessible to folded proteins; this architecture serves to prevent degradation of non-substrate proteins. After substrate binding, Lon uses the power of ATP hydrolysis coupled to conformational changes to unfold substrates (if necessary), and then to translocate the polypeptide chain through a central pore into the degradation chamber.<sup>10,11</sup> Lon often recognizes unfolded proteins via short peptide sequences (degrons) exposed in the unfolded protein that are buried and inaccessible in the folded version. The beta-20 peptide (or  $\beta$ -20), isolated from unfolded  $\beta$ -galactosidase, is an example of this type of degron.<sup>12</sup> Lon also degrades multiple other classes of substrates. In many of these instances, Lon recognizes folded proteins through unstructured peptide degrons displayed on the protein surface, such as in an exposed loop or near the termini. For example, Lon specifically recognizes the last 20 amino acids of the cell division inhibitor Sula and also the first 21 residues of the superoxide response regulator SoxS.<sup>5,13</sup> In contrast, Lon can also bind certain folded protein domains lacking any known degron peptide; this class of substrate is represented by the  $\alpha$ -crystallin domains of the small heat shock proteins (sHSPs, IbpA, and IbpB in bacteria).<sup>4</sup> Thus, the pool of Lon substrates and the

mechanisms of recognition for degradation are both important and diverse.

Each Lon monomer contains three functional sub-regions: the N domain, AAA+ ATPase module, and a protease domain. The ATPase and protease domains are the most well-conserved regions of Lon. Interestingly, the ~300 residue N domain is the most variable region in primary sequence among Lon homologs, and it is also the least well understood in function.<sup>14</sup> Multiple lines of evidence indicate a role of the N domain in mediating recognition and processing of certain Lon substrates.<sup>15-18</sup> However, the precise binding interface and molecular interactions that underlie recognition of most Lon substrates remain unknown. Furthermore, deletion of portions of the N domain can alter or ablate both ATPase and protease activity, indicating the N domain also plays a critical role in assembly and/or control of the entire machine.<sup>14,19</sup> More recently, we discovered an additional role for the Lon N domain in the *Escherichia coli* enzyme: to mediate the higher-order assembly of a Lon dodecamer.<sup>20</sup>

In this previous study, we showed that Lon homo-hexamers associate in a head-to-head fashion to form a large, ellipsoid-shaped dodecamer based on an electron microscopy reconstruction.<sup>20</sup> Modeling of the individual structural regions of Lon strongly suggested that this association is mediated by intermolecular interactions between N domains. Protein association constants and *in vivo* concentration measurements indicate that the ratio of Lon dodecamer to hexamer is likely close to equal during balanced growth and increases when *lon* gene expression is induced under stress (e.g. heat shock).<sup>20</sup> *In vitro* analysis reveals that increasing dodecamer population correlates with approximately 10-fold lower ATPase activity as well as slower degradation of certain substrates.<sup>20</sup> Other reports identified multiple binding partners that modulate Lon activity in various ways, including DNA, inorganic polyphosphate, and protein adaptors.<sup>21-24</sup> Therefore, Lon binding to itself via dodecamer formation may represent an additional mechanism by which intermolecular interactions control Lon activity or tune substrate preference in addition to these other well-studied binding effectors. In light of these findings, we designed experiments to better understand the structural basis of dodecamer formation and possible biological roles of the Lon dodecamer during different, potentially stressful, growth conditions that require pQC.

Here, we report mutagenesis and chemical cross-linking studies that identify a precise segment of the Lon N domain in mediating dodecamer assembly. Importantly, we find a Lon variant carrying mutations in this region that preferentially forms dodecamers. The Lon V217A/Q220A (Lon<sup>VQ</sup>) variant, in which residues Val217 and Gln220 that are present in a region predicted to form intermolecular coiled coils between hexamers were mutated to alanine, showed an increased propensity to form dodecamers both in solution and by EM analysis. This Lon<sup>VQ</sup> variant was analyzed biochemically as well as expressed *in vivo*. Our results indicate that the dodecamer is active, although it exhibits alterations in substrate selection and/or degradation. Similar changes in substrate choice are observed both *in vivo* and *in vitro*, strongly suggesting that Lon<sup>VQ</sup> exists largely in dodecamer form under standard growth conditions. Cells expressing only Lon<sup>VQ</sup> are healthier than Lon-deficient strains during normal growth and perform similarly to wild-type Lon in a panel of *in vivo* bioassays except for degradation of small heat shock proteins. Thus, we conclude that the dodecamer successfully completes many of the Lon protease's important regulatory functions while modifying substrate choice, perhaps to better manage protein quality control under conditions such as UV, heat, and oxidative stress.

## Results

### Identification of N domain interactions underlying Lon dodecamer formation

Our previous work identified that Lon forms a dodecamer and suggested that intermolecular N domain interactions were likely responsible. This model of Lon dodecamer assembly was constructed using low-resolution transmission electron microscopy (EM) image analysis.<sup>20</sup> The resulting ellipsoidal electron density map was sufficient to model two barrel-shaped hexamers at the distal ends of the dodecamer corresponding to the Lon ATPase and protease modules [Fig. 1(a)]. The two barrels were then bridged by six extended helical structures, which were modeled as six N domain dimers forming end-to-end interactions that mimic two-stranded, antiparallel coiled coils [Fig. 1(a)]. Although the model informs that the Lon N domains are primarily responsible for dodecamer formation, the specific intermolecular interactions necessary to stabilize this large assembly could not be obtained due to the low resolution of the EM map (~35–40 Å).<sup>20</sup> Therefore, to identify the specific residue contacts that underlie dodecamer assembly, we carried out bioinformatics analysis followed by scanning mutagenesis and crosslinking studies targeted at residues predicted to participate in N domain interactions.

Inspection of the isolated *E. coli* Lon N domain crystal structure reveals an extended  $\alpha$ -helix (Residues 189–242), which contains more than one region with a high probability of forming coiled-coil

interactions based on primary sequence analysis.<sup>25,26</sup> Using the Lon EM dodecamer model, we constrained our bioinformatics predictions to be dimeric, antiparallel, coiled coils. Candidate residues for subsequent cysteine mutagenesis and crosslinking were identified from several models predicted using Drawcoil 1.0, including Val209, Ile213, Val217, Gln220, Ser224, and Tyr228 (Fig. S1).<sup>27</sup> We purified Lon variants in the presence of reducing agent, then rapidly diluted into Lon reaction buffer containing ATP $\gamma$ S (a non-hydrolyzable ATP analog) and the oxidizing catalyst copper phenanthroline, and monitored crosslinking over time by SDS-PAGE. In the presence of the oxidizing catalyst, wild-type Lon (Lon<sup>WT</sup>), which has six cysteine residues but none located in the predicted coiled-coil region, showed no disulfide-based crosslinking [Fig. 1(b)]. In contrast, we identified two cysteine variants from the six candidates, Val217C (Lon<sup>V217C</sup>) and Gln220C (Lon<sup>Q220C</sup>), that reproducibly yielded fast and robust intermolecular disulfide crosslinking [Fig. 1(c,d)]. Dimer formation increased over time, suggesting these two residues are likely participating in the antiparallel coiled-coil interface between two Lon hexamers. Additionally, low levels of oligomerization were detected for both variants even without an oxidizing catalyst, indicating that the absence of a reducing agent alone is sufficient for spontaneous disulfide-bond formation. Finally, treatment of the oxidized samples with reducing agent resulted in a loss of the higher molecular weight species in SDS-PAGE, confirming that the cysteine-based disulfide crosslinking was responsible for the formation of the SDS-resistant dimers. A model of an antiparallel coiled coil that is consistent with our results and the corresponding bioinformatics helical wheel diagram are shown in Figures 1(e) and S1.

### Mutation of Val217 and Gln220 shifts Lon population toward dodecamer

To further probe the role of residues Val217 and Gln220 in dodecamer formation and stabilization, both residues were mutated to alanines, and the resulting variant (Lon V217A/Q220A, henceforth Lon<sup>VQ</sup>) was characterized biophysically using analytical ultracentrifugation (AUC). Our previous study showed Lon<sup>WT</sup> sediments as a mixture of oligomer assemblies, and the percentage of dodecamer in the population increases with concentration.<sup>20</sup> Due to the interconversion between hexamer and dodecamer, all future references to Lon concentration will be in monomer equivalents. Both Lon<sup>WT</sup> and Lon<sup>VQ</sup> were assayed using sedimentation velocity AUC at multiple concentrations in the presence of ATP $\gamma$ S (Fig. 2). The previously calculated dissociation constant between dodecamer and hexamer for Lon<sup>WT</sup> was approximately 1–3  $\mu$ M (monomer equivalents). Interestingly, Lon<sup>VQ</sup> also sediments as a mixture of

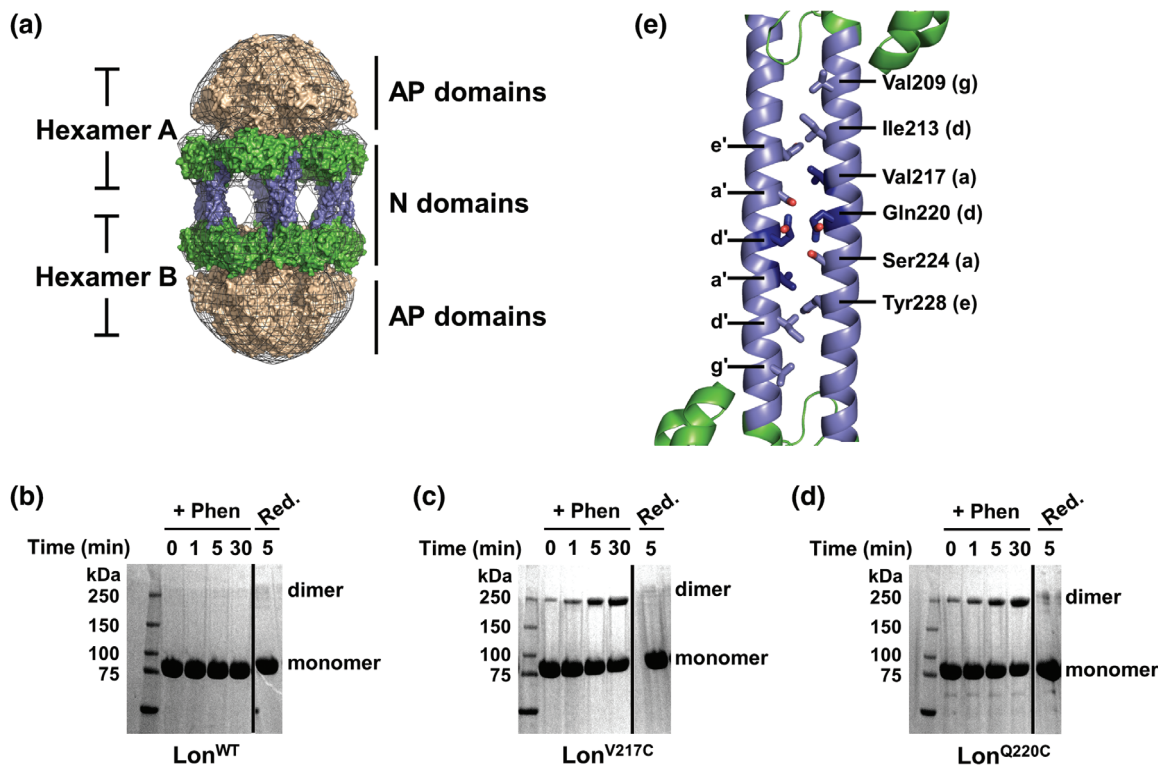


**Figure 1.** The Lon dodecamer forms via putative N domain coiled-coil interactions. (a) Low-resolution electron microscopy 3D reconstruction presents a model for dodecamer formation via the association of Lon N domains through antiparallel coiled coils. Lon N domain dimers are in green with the predicted coiled-coil region colored blue, the hexameric ATPase and protease domains are colored tan, and the electron density map is shown as a gray mesh. Details for model reconstruction were described previously<sup>20</sup>. (b–d) Copper phenanthroline catalyzed crosslinking of Lon<sup>WT</sup> and Lon variants analyzed by SDS-PAGE. Lon proteins (20  $\mu$ M) were incubated with catalyst (+Phen) for the indicated times, then reduced with 10 mM  $\beta$ -mercaptoethanol and 5 mM DTT (Red.). Lon<sup>WT</sup> (b) shows no crosslinking in the presence of phenanthroline whereas Lon<sup>V217C</sup> (c) and Lon<sup>Q220C</sup> (d) both show a time-dependent increase in crosslinking with oxidizing agent. All crosslinking was abolished by addition of reducing agent. Solid line indicates a portion of the gel that was removed for clarity. (e) Bioinformatics analysis was used to create a theoretical model of the Lon N domain antiparallel coiled-coil interactions (cartoon representation, colored as in (a)). The residues chosen for mutagenesis (shown in stick representation) were mapped on the *E. coli* Lon N domain structure (PDB 3LJC). Two Lon N domain monomers were manually modeled in an antiparallel conformation to mimic the potential interaction surface and residues Val217 and Gln220 are highlighted in dark blue. The lower case letters denote the coiled-coil heptad position as displayed in Fig. S1.

hexamer and dodecamer, however, this variant exhibited a higher percentage of dodecamer populated compared with Lon<sup>WT</sup> at all concentrations tested. Importantly, at lower concentrations (e.g. 3 and 1.5  $\mu$ M) where Lon<sup>WT</sup> is presumed to be predominately hexamer, Lon<sup>VQ</sup> is still predominately dodecamer and the relative amount of dodecamer increases with increasing concentration. At the concentration where Lon<sup>WT</sup> approximately equally populated the hexamer and dodecamer, Lon<sup>VQ</sup> was calculated to be over 75% dodecamer. Furthermore, at the highest concentration assayed, Lon<sup>VQ</sup> was more than 90% dodecamer. Using these data, the Lon<sup>VQ</sup> variant was calculated to have a dissociation constant of  $\sim 0.5 \pm 0.1 \mu$ M, about 5-fold tighter than that of Lon<sup>WT</sup> (see Materials and Methods). Therefore, the Lon<sup>VQ</sup> variant exists predominately as a dodecamer in solution, even at concentrations where Lon<sup>WT</sup> exists mostly as a hexamer.

Next, we analyzed the oligomeric propensity of the Lon<sup>VQ</sup> variant using EM (Fig. 3). Both Lon<sup>WT</sup> and Lon<sup>VQ</sup> samples were diluted to the same starting concentration, which populates primarily dodecamers for both variants (11  $\mu$ M monomer). The samples were incubated at 37°C with ATP and MgCl<sub>2</sub>, then the reaction quenched with ATP $\gamma$ S. Samples were diluted to 340 nM, immediately immobilized on grids, and stained with uranyl acetate before imaging. Individual hexamer and dodecamer particles were chosen over multiple images and quantified. Lon<sup>WT</sup> EM images displayed approximately 43% hexamer and 57% dodecamer particles. Under the same experimental conditions and protein concentrations, the Lon<sup>VQ</sup> particles were approximately 21% hexamer and 79% dodecamer. Although this procedure is not a true equilibrium experiment as time of dilution, the grid surface, and a capacity of being able to more easily identify some types of particles than others could all

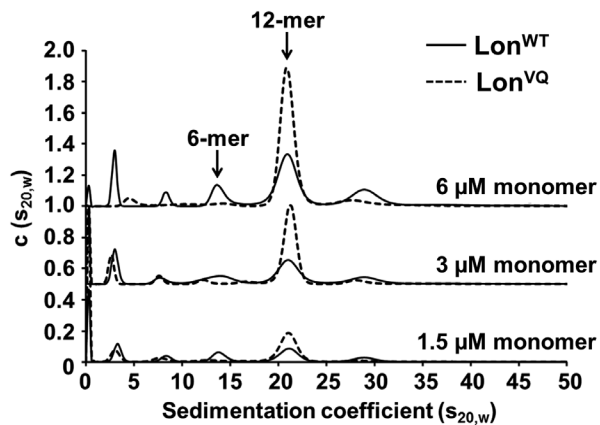


**Figure 2.** Lon<sup>VQ</sup> preferentially forms dodecamers in solution. Sedimentation velocity analytical ultracentrifugation of Lon<sup>WT</sup> (solid line) and Lon<sup>VQ</sup> (dashed line). Sedimentation analysis shows the Lon<sup>VQ</sup> variant forms a higher percentage of dodecamers in solution. The population of dodecamer increases with concentration for both Lon variants; however, at each concentration shown, there is a higher dodecamer population for Lon<sup>VQ</sup> compared with Lon<sup>WT</sup>. The  $c(s_{20,w})$  values for each concentration series were offset by a standard value for clarity.

influence the quantification. Nonetheless, this EM characterization confirms the crosslinking experiments presented above in identifying Lon residues Val217 and Gln220 as being involved in dodecamer stabilization.

### Lon<sup>VQ</sup> displays biochemical activities comparable to the Lon<sup>WT</sup> dodecamer

Previous studies revealed that Lon's intrinsic ATPase activity (not stimulated by protein substrate) decreases with increasing protein concentration and the coincident dodecamer formation.<sup>20</sup> Based on these basal

ATPase activities, the Lon dodecamer hydrolyzes ATP approximately 10-fold slower than the hexamer. We assayed ATPase activity for Lon<sup>VQ</sup> at concentrations in which Lon<sup>WT</sup> was either predominately hexamer or predominately dodecamer (each with the same number of monomer equivalents) [Fig. 4(a)]. At lower concentrations where Lon<sup>WT</sup> is mostly hexamer (0.75 μM), Lon<sup>VQ</sup> displayed an approximately 1.5-fold slower basal ATPase activity. As the concentration of Lon increases, so does the amount of dodecamer present in the sample. At 12 μM Lon monomer, where the majority of Lon<sup>WT</sup> is predicted to be dodecamer, Lon<sup>VQ</sup> had nearly identical ATPase activity compared with Lon<sup>WT</sup>. Notably, at monomer concentrations at or below the dissociation constant for Lon<sup>WT</sup>, Lon<sup>VQ</sup> had depressed ATPase activity compared with Lon<sup>WT</sup>. These activity assays thus confirm our previous biophysical studies that reveal that Lon<sup>VQ</sup> has a tighter hexamer–dodecamer equilibrium. We also assayed substrate-stimulated ATPase rates using an unfolded substrate with a Lon-specific degron (Fig. S2). While both Lon<sup>WT</sup> and Lon<sup>VQ</sup> displayed higher ATPase activity in the presence of substrate, there was still a concentration-dependence in activity, indicating that substrate-binding does not lead to dodecamer dissociation.

We also assayed *in vitro* degradation of two classes of radiolabeled model Lon substrates by monitoring generation of acid-soluble peptides with time over a range of Lon<sup>WT</sup> or Lon<sup>VQ</sup> concentrations that would contain different percentages of dodecamer. First, we monitored the degradation of Sula as a representative of small folded substrates. Sula is induced during the SOS response to DNA-damage to allow for DNA repair prior to cell division. After stress, Lon specifically degrades Sula via recognition of a short unstructured C-terminal tail (sul20, residues 150–169) with a  $K_m$  of approximately 40 μM.<sup>5,12,28</sup>

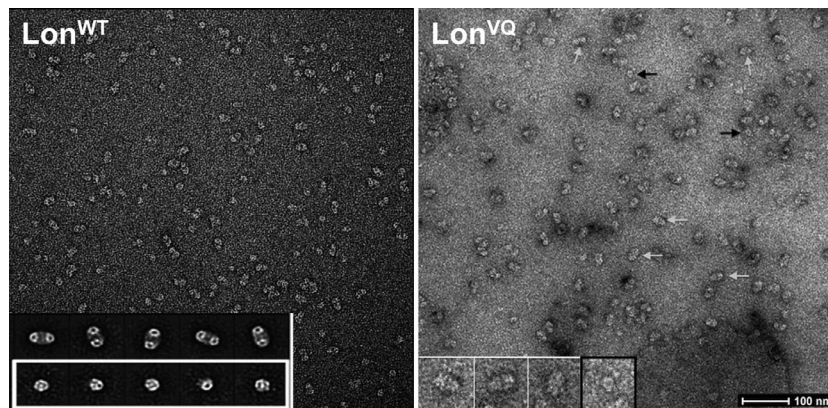


**Figure 3.** Electron microscopy analysis and quantification of Lon<sup>VQ</sup> dodecamer formation. Negative stain electron micrographs of Lon<sup>WT</sup> (left) and Lon<sup>VQ</sup> (right). Under the same experimental conditions and upon immobilization on the grids, Lon<sup>VQ</sup> forms a higher percentage of dodecamers. Representative dodecamer and hexamer particles are denoted with white and black arrows, respectively. Inset left: representative class images of dodecamers (top) and hexamers (bottom) based on the Lon<sup>WT</sup> negative stain particles.<sup>20</sup> Inset right: zoomed in view of raw Lon<sup>VQ</sup> particles. The three particles on the left in white boxes are dodecamers and the particle on the right in the black box is a representative hexamer. Scale bar shown represents 100 nm.

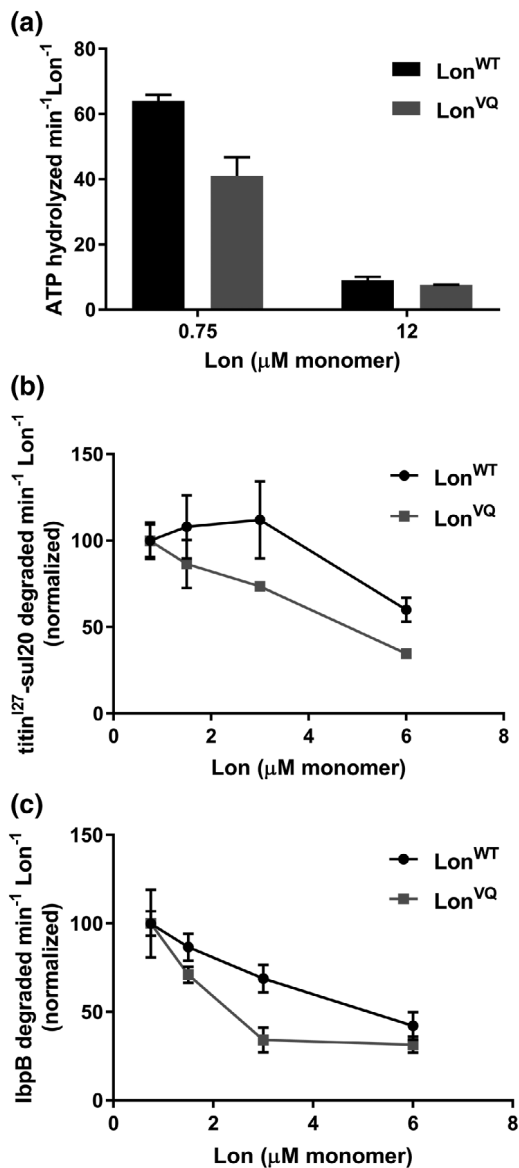


**Figure 4.** Lon<sup>VQ</sup> displays diminished ATPase and degradation activity compared with Lon<sup>WT</sup>. (a) ATP hydrolysis activity of Lon<sup>WT</sup> (dark gray bars) and Lon<sup>VQ</sup> (light gray bars). At lower concentrations where Lon<sup>WT</sup> is predominately hexameric, there is approximately 1.5-fold higher activity for Lon<sup>WT</sup> compared with Lon<sup>VQ</sup>. However, at higher concentrations where both proteins are expected to be predominantly dodecamer, the ATP hydrolysis activity is comparable. The values reported are from three independent experiments performed in triplicate, and the error bars represent SEM. (b and c) Degradation of 40  $\mu\text{M}$  <sup>35</sup>S-titin<sup>I27</sup>-sul20 (b) and <sup>35</sup>S-IbpB (c) by Lon<sup>WT</sup> and Lon<sup>VQ</sup> was monitored by generation of acid-soluble radioactive peptides. The indicated Lon concentrations are in monomer equivalents. Degradation rates were normalized in comparison to the rate at 0.75  $\mu\text{M}$ . Each experiment was performed in triplicate and error bars represent SEM (curved lines connecting data points do not represent statistically-based fitting).

We appended the Sula degron onto the C-terminus of the I27 domain of human titin (titin<sup>I27</sup>-sul20, approximately 14 kDa). Increasing concentrations of Lon<sup>VQ</sup>

caused a larger decrease in proteolytic activity compared with Lon<sup>WT</sup>, and at the highest concentration assayed, the Lon<sup>VQ</sup> degradation rate was significantly (1.8-fold) slower than Lon<sup>WT</sup> [Fig. 4(b)]. We also assayed processing of the sHSP IbpB, which readily forms oligomers (tetramers and greater) under our experimental conditions, making it a larger substrate than the titin<sup>I27</sup> domain. Lon<sup>WT</sup> recognizes IbpB via its folded  $\alpha$ -crystallin domain with a  $K_m$  of 16  $\mu\text{M}$ .<sup>4</sup> Lon<sup>VQ</sup> was able to degrade the oligomeric IbpB *in vitro*, however at a much slower rate than Lon<sup>WT</sup> [Fig. 4(c)]. Again, increasing Lon<sup>VQ</sup> concentration had a greater effect on diminishing degradation activity for IbpB compared with Lon<sup>WT</sup>, similar to the processing of the titin<sup>I27</sup>-sul20 substrate. The concentration range over which Lon<sup>VQ</sup> showed slowed degradation was significantly lower than was observed with Lon<sup>WT</sup>. Thus, as with the intrinsic ATPase rates, protein degradation rates, especially of IbpB, appear to serve as a surrogate for measuring the amount of the Lon dodecamer population at each concentration. These observations support the conclusion that Lon<sup>VQ</sup> hexamers and dodecamers behave similarly to Lon<sup>WT</sup> except for exhibiting a shifted hexamer-dodecamer equilibrium constant to a lower (tighter) value.

#### **Lon<sup>VQ</sup> is altered in recognition of dodecamer-sensitive substrates *in vivo***

We established *in vitro* that a hallmark of the Lon dodecamer is a diminished rate of IbpB degradation (this work and Refs. [20]). Therefore, using this phenotype as a measure of dodecamer population, we sought to assay the assembly and activity of Lon<sup>VQ</sup> *in vivo* by monitoring the interaction of Lon with IbpA, a paralog IbpB and also a substrate of Lon,<sup>4</sup> after heat shock. IbpA is induced to help prevent toxic aggregation of unfolded proteins during heat stress.<sup>29,30</sup> Lon recognizes the folded  $\alpha$ -crystallin domain of IbpA leading to degradation of IbpA after heat stress, allowing for release of unfolded client proteins so they are available for refolding by folding chaperones.<sup>4</sup> While both IbpA and IbpB are Lon substrates, we were constrained to follow only IbpA degradation *in vivo* due to the poor specificity of our IbpB antibodies. Although IbpA monomers are small (~16 kDa), they form large oligomers under heat stress, similar to IbpB.<sup>31,32</sup> *Escherichia coli* cultures expressing Lon<sup>WT</sup>, Lon<sup>VQ</sup> (integrated into the normal chromosomal locus) or with the endogenous *lon* gene deleted and replaced with a kanamycin-resistant cassette ( $\Delta lon$ ) were grown at 37°C and then stressed by shifting the cultures to 45°C. Cellular levels of IbpA were monitored at the indicated time points via Western blot (Fig. 5). Lon<sup>WT</sup> degrades IbpA slowly over time under heat stress ( $t_{1/2}$  ~ 30 min) with approximately 70% of the initial protein lost 45 min post heat shock. Conversely, IbpA degradation is severely

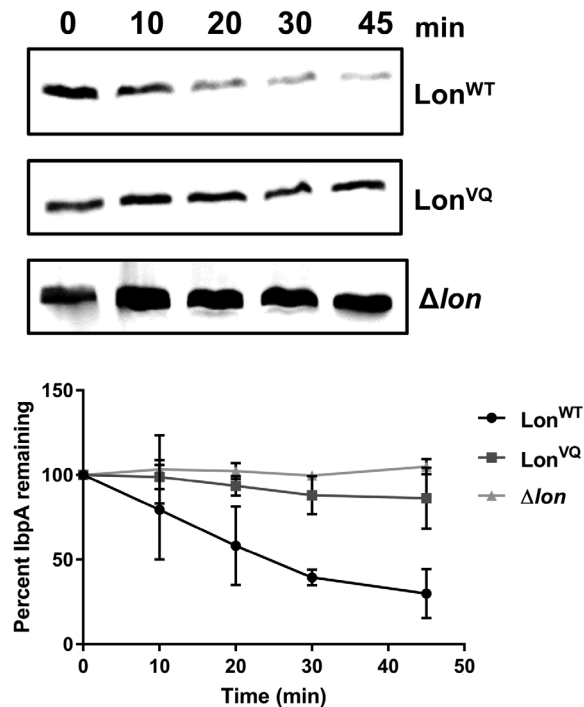


**Figure 5.** *In vivo* degradation of IbpA by Lon upon heat shock. Representative Western blots of *E. coli* cell extracts during heat shock (45°C) monitoring loss of the IbpA protein over time. *Bottom.* Protein bands were quantified and the percentage of IbpA protein remaining when Lon<sup>WT</sup> (circles), Lon<sup>VQ</sup> (squares), or Δlon (triangles) was expressed is plotted as a function of time. The experiment was performed in triplicate and error bars represent SEM (lines connecting data points are not indicative of statistically based fitting).

reduced when Lon<sup>VQ</sup> was expressed, with less than 15% of total IbpA degraded after the same time period. As a control that IbpA is normally a Lon substrate under these conditions, we observed that IbpA was stable throughout the time course when endogenous *lon* was deleted. In our previous report, we identified that cellular levels of Lon<sup>WT</sup> increase ~1.2-fold under heat stress.<sup>20</sup> However, under these conditions, there is still approximately 45% Lon<sup>WT</sup> hexamer available to degrade IbpA. With the Lon<sup>VQ</sup> variant, because it is largely dodecamer both at 37°C and 45°C, we would expect an intermediate phenotype between Lon<sup>WT</sup> (a mixture of hexamers and dodecamers) and Δlon strains, which is indeed what we found. Thus, we suggest that the increased dodecamer population in Lon<sup>VQ</sup> disrupts the ability of Lon to degrade IbpA *in vivo*. This degradation pattern by Lon<sup>VQ</sup>, taken together with our *in vitro* analysis demonstrating that a major signature of the Lon dodecamer is its slow degradation of IbpB [Fig. 4(c)], suggests that Lon<sup>VQ</sup> is largely in the dodecamer form under these growth conditions *in vivo*, whereas Lon<sup>WT</sup> has a comparatively higher hexamer population.

### Lon<sup>VQ</sup> is active *in vivo*, indicating dodecamers are a functional form of Lon

Having developed combined *in vitro* and *in vivo* evidence that Lon<sup>VQ</sup> is largely behaving as a dodecamer, we went on to investigate possible *in vivo* function(s) of the dodecamer. We started with bioassays for classically-studied substrates. First, we monitored Lon degradation of RcsA, a 24 kDa transcription factor, which normally suppresses colonic acid exopolysaccharide production.<sup>33</sup> Using the same set of isogenic *lon* strains, we assayed growth on minimal media agar plates [Fig. 6(a)]. After 4 days, there was robust overproduction of colonic acid in the Δlon strain, evidenced by mucoid colonies, indicating this strain is deficient in RcsA degradation. However, both the Lon<sup>WT</sup>- and Lon<sup>VQ</sup>-expressing strains were non-mucoid, indicating that the Lon dodecamer is competent to degrade RcsA *in vivo* and thus properly regulate exopolysaccharide production.

We next assayed *in vivo* inactivation of the cell division inhibitor Sula (19 kDa). DNA damage was introduced by a pulse of UV irradiation and then surviving cells were allowed to grow overnight on LB agar plates [Fig. 6(b)]. In the case of the Δlon strain, cells had little or no ability to form colonies after irradiation. However, strains expressing either Lon<sup>WT</sup> or Lon<sup>VQ</sup> were able to rescue the growth-arrest phenotype induced by DNA damage. This assay suggests that the Lon<sup>VQ</sup> dodecamer is capable of interacting with Sula *in vivo* in a manner leading to timely Sula inactivation and resumption of cell division. It should be noted that this assay may report on the binding of Lon to Sula, and not necessarily Sula degradation, as a catalytically inactive Lon variant in which the active-site serine is mutated to alanine (Lon<sup>S679A</sup>) is also able to suppress the growth inhibition caused by Sula.<sup>18</sup>

Finally, we monitored the growth of these strains during heat stress [Fig. 6(c)]. Cultures were grown in exponential phase to an OD<sub>600</sub> of 0.3, then transferred to 45°C and OD<sub>600</sub> measurements taken at the indicated intervals. At 37°C, the Δlon strain grew significantly slower than the other two strains and never established a true exponential phase [Fig. 6(c)]. In contrast, there was no appreciable difference between the growth rates of the *lon*<sup>WT</sup> and *lon*<sup>VQ</sup> strains, indicating that Lon dodecamers can perform the functions needed for wild-type growth efficiency at normal temperatures. Interestingly, however, after increasing temperature, the growth rates for all three strains were slower but their doubling times were similar within experimental error (~43 min). These data suggest that immediately after shifting to high temperature, loss of Lon activity is not deleterious to viability. Therefore, the lower activity of Lon dodecamers may be advantageous, as its formation prevents degradation of certain substrates, such as IbpA, IbpB,



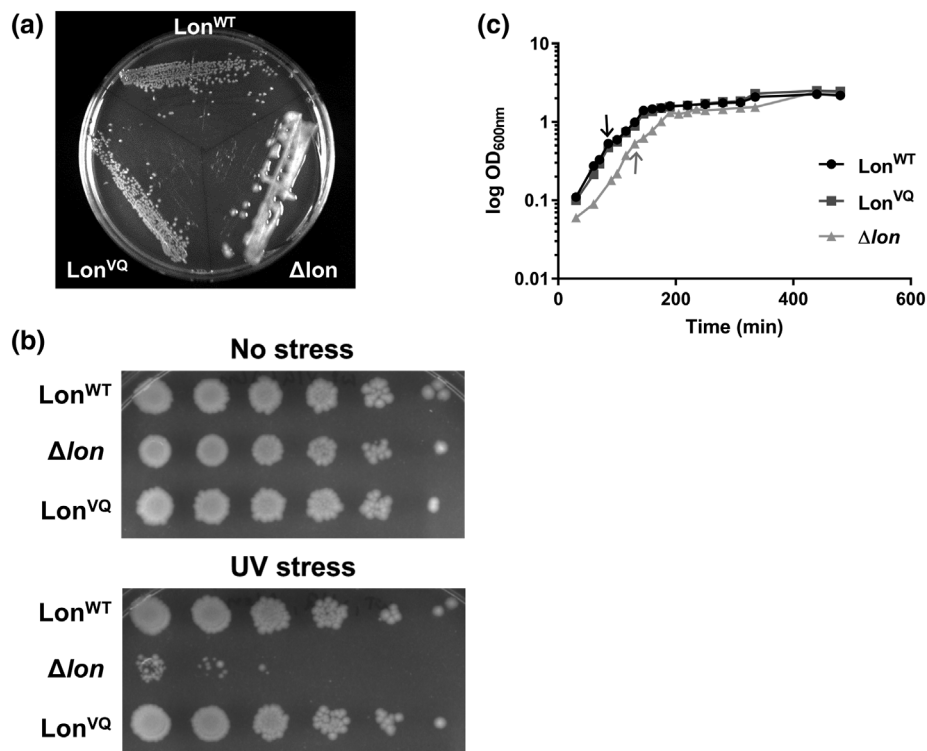


**Figure 6.** Lon<sup>VQ</sup> is functional *in vivo*. (a) W3110 *E. coli* cells expressing either Lon<sup>WT</sup> or Lon<sup>VQ</sup> from the endogenous *lon* locus or with the genomic *lon* copy deleted and replaced with a kanamycin-resistant cassette ( $\Delta lon$ ) were grown in culture then plated on M9 minimal media agar plates. Lon degradation of RcsA reduces colonic acid synthesis. Stabilization of RcsA in  $\Delta lon$  strain results in a mucoid phenotype. (b) *In vivo* bioassay monitoring inactivation of the cell division inhibitor protein SulA by Lon after UV stress. Lon<sup>WT</sup> is able to inactivate SulA which allows for cell division and growth after UV irradiation (top row). However, when Lon is deleted (middle row), cells are unable to recover from UV damage. Expression of Lon<sup>VQ</sup> from the endogenous locus is also able to allow for cell growth recovery after UV stress similar to Lon<sup>WT</sup>. Each column, from left to right, represents a 10-fold serial dilution. (c) Growth curves of isogenic *lon* W3110 strains. The  $\Delta lon$  strain grew significantly slower than Lon<sup>WT</sup> and Lon<sup>VQ</sup> (student's unpaired t test,  $P > 0.0005$  and  $0.005$  for Lon<sup>WT</sup> and Lon<sup>VQ</sup>, respectively) at 37°C; however, all strains had similar growth rates at 45°C (temperature shift indicated by black arrow for Lon<sup>WT</sup> and Lon<sup>VQ</sup> or gray arrow for  $\Delta lon$ ). Each semi-log plot is the average of two independent cultures and error bars represent SEM.

and perhaps others. A switch to low temperature and recovery from heat stress would then require the activity of the Lon hexamer to degrade these regulatory proteins that are no longer needed.

## Discussion

Lon protease plays a major role in maintaining pQC in bacteria as the primary protease responsible for degrading unfolded or damaged proteins that result from various cellular stresses. Previous studies characterized Lon to function as a homo-hexamer with the proteolytic active sites sequestered in a cavity that is accessed through a small central pore. More recently, our group found that Lon hexamers associate in a head-to-head orientation to form a larger ellipsoidal-shaped dodecamer. Using the available crystal structures of individual Lon domains<sup>25,34</sup> together with bioinformatics, we proposed and then tested if this association was mediated by antiparallel coiled coils between opposing Lon N domains, canonical interaction motifs that underlie oligomerization of many proteins.<sup>35</sup> *In vitro* we demonstrated that the

dodecamer is increasingly populated with increasing Lon concentration. Based on the determined  $K_D$  for assembly and the cellular Lon concentration, we predicted that Lon exists in equilibrium between the hexamer and dodecamer forms in wild-type cells *in vivo*.<sup>20</sup> Importantly, the Lon dodecamer displays decreased ATPase activity as well as differences in substrate processing *in vitro* compared with the Lon hexamer. As such, we sought to further characterize Lon to advance understanding of the dodecamer form and uncover possible biological functions of this assembly state during pQC and stress responses.

The major impediment to elucidating the biological function of the Lon dodecamer is the inability to isolate a homogeneous population of this assembly using wild-type protein. Further limiting experimental approaches, the precise molecular contacts required for dodecamer formation were unknown. Therefore, we employed computation-directed mutagenesis, protein-protein crosslinking, and biochemical analysis to identify a variant of Lon that prefers the dodecameric state. We identified that Lon N domain residues



Val217 and Gln220 are featured at the oligomerization interface based on the results of cysteine mutagenesis and disulfide-based crosslinking. Interestingly, when both residues are mutated to alanine, presumably removing wild-type hydrophobic or polar interactions between the antiparallel coils, the dodecamer is stabilized compared with that of Lon<sup>WT</sup>. These mutations result in an increased percentage of dodecamer at physiological protein concentrations, as observed by analytical ultracentrifugation. This increased propensity to form dodecamers was confirmed using electron microscopy. We hypothesize the alanine mutations may have disrupted the natural balance of intermolecular interactions that allow for rapid interconversion between the hexameric and dodecameric forms in favor of a tighter dodecamer interface. As predicted from its increased dodecamer stability, Lon<sup>VQ</sup> is less active at low concentrations compared with Lon<sup>WT</sup>, an additional indicator of a larger dodecamer population. Importantly, based on the hexamer–dodecamer  $K_d$  of 0.5  $\mu\text{M}$  for Lon<sup>VQ</sup>, this newly identified variant is predicted to exist as majority dodecamer *in vivo*, as the intracellular Lon concentration was determined to be approximately 2.5  $\mu\text{M}$  monomer.<sup>20</sup>

It should be noted that although the Lon<sup>VQ</sup> variant is largely dodecamer at all concentrations assayed *in vitro*, these samples are not homogeneous, as a small fraction of hexamers remain. This mixture is evidenced by the concentration dependence of the ATPase activity and *in vitro* substrate degradation rates, a behavior that was also seen for Lon<sup>WT</sup>, albeit over a higher concentration range. Additionally, quantification of EM particles reports approximately 20% of the total Lon<sup>VQ</sup> population is hexameric after immobilization on grids. Nevertheless, the combination of these mutations yielded a Lon variant with an approximate 5-fold tighter dissociation constant for dodecamer formation compared with Lon<sup>WT</sup>. Therefore, we have improved our understanding of how the dodecamer is formed by identifying (i) the N domain antiparallel coiled-coil register, (ii) a critical part of the intermolecular interaction interface that mediates dodecamer assembly as well as (iii) generating a molecular tool to more clearly test the activities and *in vivo* functions of the dodecamer.

A previous study identified a separate mutation in the Lon N domain that also yields a Lon population that is primarily dodecamer.<sup>17</sup> It was reported that the Glu240 to Lys mutation (Lon<sup>E240K</sup>) results in a Lon dodecamer dissociation constant of 2.6 nM, an approximately 1000-times tighter interaction than that of Lon<sup>WT</sup>.<sup>17</sup> Residue 240 is located in the second of the two predicted coiled-coil regions in the Lon N domain (coiled-coil Region 1 is comprised of Residues 185–228 and Region 2 is composed of Residues 230–278). We chose to focus on mutations solely in the first predicted coiled-coil region for multiple reasons. First, the Lon<sup>E240K</sup> variant has altered substrate

specificity as evidenced by the finding that the recognition and the degradation of the RcsA substrate by Lon<sup>E240K</sup> are diminished while SulA substrate recognition is unaffected.<sup>15</sup> Also, biochemical evidence suggested the Lon<sup>E240K</sup> dodecamer might be allosterically regulated in a different manner compared with the Lon<sup>WT</sup> dodecamer. For example, Lon<sup>E240K</sup> dodecamers degraded the model Lon substrate casein nearly as efficiently as the Lon<sup>WT</sup> hexamer, whereas dodecamers formed by Lon<sup>WT</sup> or Lon<sup>VQ</sup> subunits behave similarly and degrade this substrate very slowly.<sup>17</sup> Finally, other reports identified that the N domain region containing Residues 240–252 is important for proper ATPase activity, substrate translocation, and degradation.<sup>19</sup> Therefore, we chose to focus this study on N domain residues upstream of this allosteric regulatory region in order to minimize potential confounding effects that could interfere with the unambiguous elucidation of dodecamer function.

Among Lon homologs, the N domain is the most variable region, compared with the ATPase and protease domains. Despite lower sequence homology, dimerization of N domains via coiled-coil interactions seems to be a conserved feature among Lon homologs.<sup>15,34,36,37</sup> However, there may be additional regions other than the segment probed in this study that could mediate antiparallel coiled-coil formation.<sup>15,36</sup> Interestingly, *E. coli* Val217 is conserved among proteobacteria whereas Gln220 is slightly more variable. Therefore, it will be worthwhile to determine if other Lon homologs also form larger assemblies. If so, dodecamer formation may be a conserved mechanism to regulate Lon protease function. Based on experiments with *Bacillus subtilis* Lon, it was suggested this homolog also forms larger assemblies in solution as the N domains dimerize via coiled-coil interaction.<sup>34</sup> Preliminary experiments in our lab also detected a dodecamer-like species with this full-length protein.

There is increasing evidence to support the theory that coiled-coil interactions may be a conserved feature of several AAA+ pQC enzymes. Although there is likely some diversity in the orientation of these interactions, it seems higher-order assembly is a mechanism for modulating activity. For instance, the coiled-coil middle domains (MD) of the ClpB disaggregase interact in a head-to-tail orientation, leading to suppression of ATPase activity.<sup>38,39</sup> Disruption of these interactions by binding of the DnaK co-chaperone, in turn, alleviates the suppression, allowing for normal ClpB activity.<sup>40</sup> Another AAA+ chaperone ClpC was recently shown to also oligomerize via coiled-coil MD interactions, but in this instance in a head-to-head orientation, as we find for *E. coli* Lon.<sup>41</sup> Binding of the MecA adaptor to the MD results in conformational changes that break the coiled-coil interactions leading to stabilization of active ClpC hexamers. The differentiating feature of the Lon

dodecamer is that it does not appear to be an inactive “storage form” of Lon preventing degradation of substrates, and we did not identify substrate interactions that altered assembly. For example, previous negative stain EM micrographs, taken in the presence of a SulaA degron peptide, still contained a significant dodecamer population.<sup>20</sup> Also, the Lon<sup>VQ</sup> dodecamer variant is sufficiently active in a series of *in vivo* bioassays, including suppression of extracellular capsular polysaccharide production and re-establishing cell division during recovery from DNA damage. Rather, our results suggest that the Lon dodecamer may be unable to degrade larger substrates like the oligomers formed by the Ibps,<sup>42</sup> but still able to degrade smaller (<25 kDa) substrates relatively well, such as RcsA and Sula (this work) as well as small degron-tagged model proteins.<sup>20</sup> The Lon dodecamer’s inability to degrade IbpA during growth at high temperature *in vivo* may be important to allow efficient IbpA binding to aggregating client proteins during heat shock. Then, once cells return to a lower stress environment, the Ibp–client complexes are likely preferential substrates for disaggregation and refolding. Thus, unlike ClpB or ClpC, Lon dodecamer formation may be a way to tune, but not preclude, substrate recognition and subsequent degradation in the presence of cellular stress. Because Lon has such a large number of substrates that must be degraded under specialized conditions, such tuning rather than inactivation may be advantageous to cells.

Several questions about the role of Lon dodecamer formation *in vivo* remain to be addressed. For instance, could certain substrate and small molecule binding sites located on the N domain become occluded upon dodecamer assembly? Also, could the altered “resting” ATPase activity of the dodecamer play a role in slowing or preventing substrate processing during cellular stress when certain Lon substrates are needed for their anti-aggregation function? These questions can now be dissected using this Lon<sup>VQ</sup> dodecamer-favoring variant using a combined *in vivo* and *in vitro* approach. Commensurate with our understanding of the biological significance of the Lon dodecamer, the next step in understanding Lon function *in vivo* is to develop variants of Lon that form obligate hexamers to compare to our current data. However, this endeavor may prove to be precarious, especially if dodecamer formation is a key mechanism for controlling deleterious proteolysis of critical Lon substrates in response to specific environmental conditions.

## Materials and Methods

### Protein expression and purification

Wild-type Lon and Lon N domain variants were expressed and purified as previously described.<sup>20</sup> Briefly, Lon was cloned into the pBAD33 vector and

all Lon variants were produced with the QuikChange site-directed mutagenesis protocol (Agilent) using specific primers containing the desired mutations. Proteins were grown in TB media at 37°C and expression induced with 0.2% L-arabinose for 3–4 h followed by centrifugation to collect cell pellets. For purification, cells were resuspended in phosphate binding buffer (100 mM potassium phosphate, pH 6.5, 10% glycerol, 1 mM DTT, 1 mM EDTA) and lysed via French Press. After incubation with benzonase (25U), the lysate was clarified by centrifugation and the supernatant incubated with phosphocellulose resin (Whatman). The bound protein was eluted with 400 mM potassium phosphate, concentrated and subjected to gel filtration in high salt buffer (GE Superose 6 10/300, 25 mM Hepes pH 7.5, 2 M NaCl, 10% glycerol, 1 mM DTT, 1 mM EDTA). The appropriate protein fractions were pooled and concentrated while exchanging into Lon Storage Buffer (50 mM Hepes pH 7.5, 150 mM NaCl, 10% glycerol, 0.1 mM TCEP, 1 mM EDTA) then frozen in liquid nitrogen and stored at –80°C. All Lon concentrations are expressed in monomer equivalents using the extinction coefficient of 46,300 M<sup>-1</sup> cm<sup>-1</sup> at 280 nm. <sup>35</sup>S-labeled substrates were expressed and purified as previously described.<sup>4</sup>

### Disulfide crosslinking

The Lon cysteine variants were exchanged into pre-crosslinking buffer (50 mM Hepes, pH 7.6, 150 mM NaCl, 10% glycerol, 0.1 mM TCEP) using a PD-10 desalting column (GE Healthcare) and then concentrated (Amicon). Before starting the reaction, all proteins were diluted (approximately 1.3–3.2-fold) to 200 μM in the pre-crosslinking buffer. The reaction began by diluting Lon to 20 μM in crosslinking buffer (50 mM Hepes, pH 7.6, 150 mM NaCl, 10% glycerol) along with 2.5 mM ATPγS, 5 mM MgCl<sub>2</sub>, and crosslinking catalyst containing 5 μM cupric sulfate and either 10 μM phenanthroline or 1% DMSO. All reactions were carried out at 22°C and were quenched with 10 mM EDTA at the indicated time points. After 30 min, the samples were treated with 5 mM DTT and 10 mM β-mercaptoethanol and incubated at 95°C for 5 min to reduce disulfide bonds formed during the oxidation reaction. Samples were mixed with SDS-PAGE loading dye without reducing agent and efficiency of crosslinking analyzed by electrophoresis on a 4–15% acrylamide gel (Bio-Rad).

### Negative stain electron microscopy

Lon protein samples were first diluted to 1 mg/mL in EM buffer (50 mM Hepes pH 7.5, 150 mM NaCl, 0.1 mM TCEP, 0.01 mM EDTA) and filtered with a 0.1 μM inorganic filter (Whatman). Prior to setting up grids, Lon was incubated with ATP and MgCl<sub>2</sub> at 37°C. After 5 min, the reaction was quenched with ATPγS. Lon was diluted 0.03 mg/mL in dilution

buffer (50 mM Hepes pH 7.5, 150 mM NaCl, 0.1 mM TCEP, 0.01 mM EDTA, 10 mM MgCl<sub>2</sub>, 5 mM ATP<sub>γ</sub>S) immediately prior to spotting on grid. The diluted Lon samples were immobilized on copper mesh grids (Pacific Grid-Tech) washed with dilution buffer and the grids were subsequently stained with 2% uranyl acetate. Images were obtained with the FEI Technai Spirit Transmission Electron Microscope. For quantification of hexamer versus dodecamer population, a total of 233 and 193 particles were chosen for Lon<sup>WT</sup> and Lon<sup>VQ</sup>, respectively.

**Analytical ultracentrifugation.** Lon<sup>WT</sup> and Lon<sup>VQ</sup> protein samples were exchanged into AUC buffer (50 mM Hepes pH 7.5, 150 mM NaCl, 0.1 mM TCEP, 0.01 mM EDTA) via overnight dialysis. Both proteins were filtered and diluted to the indicated concentrations using dialysis buffer and each sample, along with the corresponding buffer reference, was supplemented with 1 mM MgCl<sub>2</sub> and 0.1 mM ATP<sub>γ</sub>S. Sedimentation velocity centrifugation using interference optics was performed with the Beckman Optima XL-1 analytical ultracentrifuge at 20°C and 20,000 rpm. Data were analyzed with Sedfit to calculate the continuous distribution of sedimentation coefficients from 1S to 60S at a resolution of 200 scans per concentration with a confidence level (*F*-ratio) of 0.95.<sup>43</sup> Calculations were performed using a density of 1.00831, a viscosity of 0.010475, and a Lon partial specific volume of 0.7431 as determined by SEDNTERP (Biomolecular Interaction Technologies Center at the University of New Hampshire; [http://bitwiki.sr.unh.edu/index.php/Main\\_Page](http://bitwiki.sr.unh.edu/index.php/Main_Page)). The dissociation constants for the dodecamer to hexamer transition for Lon<sup>WT</sup> and Lon<sup>VQ</sup> were calculated in Kaleidagraph (Synergy Software) with the equation  $y = x / (x + K_d)$ , where *y* is the fraction of dodecamer and *x* is the concentration of Lon monomer.

**ATP hydrolysis activity assays.** ATP hydrolysis activity was monitored at 37°C using an NADH-coupled assay.<sup>44</sup> Briefly, Lon protein samples were diluted serially using Lon storage buffer. The ATP regeneration mix was prepared with Lon reaction buffer (25 mM Tris pH 8, 100 mM KCl, 10 mM MgCl<sub>2</sub>, 1 mM DTT), 0.7 mM NADH, 4 mM ATP, 2% DMSO, 4 mM phosphoenolpyruvate, 13 U/mL pyruvate kinase, and 17 U/mL lactate dehydrogenase and was warmed to 37°C. The protein was added to a 384-well clear-bottom plate (Corning) in triplicate and the reaction was started by adding ATP regeneration mix to each well with a repeat pipettor. The loss of absorbance at 340 nm over time was monitored using a UV/Vis spectrometer (Molecular Devices).

#### **SulA inactivation assay**

*Escherichia coli* strain W3110 expressing wild-type Lon, Δlon::kan<sup>R</sup> or lon::lon<sup>V217A/Q220A</sup> from the

endogenous Lon promoter were grown in LB broth to an OD<sub>600</sub> of 0.9–1.3, diluted into fresh LB broth to an OD<sub>600</sub> of 0.25, and 10-fold serial dilutions were prepared. Ten microliters of each dilution were spotted onto an LB-agar plate. The plate was exposed to 254 nm UV light for 5 s and incubated overnight in the dark at 37°C.

#### **IbpA in vivo degradation assay**

*In vivo* degradation assays were performed as previously described.<sup>4</sup> Briefly, LB cultures were grown at 37°C in a shaking water bath to an OD<sub>600</sub> of 0.2. The culture was then transferred to 45°C for 30 min. A 900 μL aliquot of the culture was added to 100 μL 100% trichloroacetic acid (TCA) for the 0 min time point sample. Spectinomycin (400 μg/mL) was added, and samples were taken at 15 min intervals for 60 min while maintaining the cultures at 45°C. For each sample, OD<sub>600</sub> was determined and then TCA was added to a final concentration of 10%. Samples were centrifuged and the pellets were rinsed with acetone and suspended in 2× Tris-tricine sample buffer to normalize the cell density. An equal volume of each sample was run on a 12% Tris-tricine polyacrylamide gel. IbpA levels were detected using the anti-IbpA antibody (1:2000 dilution) and were quantified using ImageQuant software (GE Health Sciences).

#### **IbpB and titin<sup>I27</sup>-sul20 in vitro degradation assay**

*In vitro* degradation reactions using 40 μM radiolabeled substrates were performed as previously described.<sup>20</sup> IbpB degradation reactions contained 60% (vol/vol) IbpB storage buffer (50 mM Hepes-KOH [pH 8], 600 mM potassium glutamate, 20% sucrose, 0.1 mM TCEP), 5% (vol/vol) Lon storage buffer, 5 mM MgCl<sub>2</sub>, 5 mM KCl, and 2% (vol/vol) DMSO. The degradation reactions were initiated by the addition of an ATP-regeneration system, containing a final concentration of 4 mM ATP, 100 mg/mL creatine kinase, and 10 mM creatine phosphate. Degradation was monitored at 37°C by the formation of TCA-soluble radioactive peptides, as previously described.<sup>4,45</sup> Degradation of titin<sup>I27</sup>-sul20 was carried out at 37°C in buffer containing 25 mM Tris-HCl, pH 8.0, 100 mM KCl, 10 mM MgCl<sub>2</sub>, 1 mM DTT, 2 mM ATP, 100 mg/mL creatine kinase, and 10 mM creatine phosphate. Kinetics were determined using a mixture of 5% (mol/mol) <sup>35</sup>S-labeled substrate and 95% (mol/mol) unlabeled substrate, as previously described.<sup>45</sup>

#### **Mucoid phenotype assay**

LB cultures (30 mL) were inoculated with 500 μL of overnight W3110 starter culture, either wild type, or Δlon::kan<sup>R</sup> or lon::lon<sup>V217A/Q220A</sup> and grown at 37°C to an OD<sub>600</sub> of 0.8–1.0. Cultures were diluted with LB to OD<sub>600</sub> 0.25, which was further diluted 1:1000 with LB and 10 μL plated on M9 minimal media agar

plates supplemented with 1 mM magnesium sulfate, 0.05% thiamine hydrochloride, 0.004% casamino acids, and 0.2% glucose. Plates were incubated at 37°C for approximately 18 h, then at 22°C for an additional 72 h before imaging.

### W3110 *E. coli* growth curves

Duplicate LB cultures (50 mL) were inoculated with 500 µL of overnight starter culture of W3110 wild type,  $\Delta lon::kan^R$  or  $lon::lon^{V217A/Q220A}$  and grown at 37°C to OD<sub>600</sub> of 0.3. At this point, cultures were transferred to a 45°C water bath with shaking and samples removed at the indicated time points for OD measurements.

### Acknowledgments

This investigation was supported in part by a grant from The Jane Coffin Childs Memorial Fund for Medical Research (61-1529) and a Burroughs Wellcome Postdoctoral Enrichment Program Fellowship Award 1015092 (B.L.B.), a National Institutes of Health National Research Service Award postdoctoral Fellowship F32GM094994 (E.F.V.), and the Howard Hughes Medical Institute. T.A.B. and S.K. are employees of the Howard Hughes Medical Institute. Analytical Ultracentrifugation data was collected at the MIT Biophysical Instrumentation Facility for the Study of Complex Macromolecular Systems (NSF-0070319). Electron microscopy data were obtained at the W.M. Keck Biological Imaging Facility, Whitehead Institute.

### References

- Gottesman S (1996) Proteases and their targets in *Escherichia coli*. *Annu Rev Genet* 30:465–506.
- Wang N, Gottesman S, Willingham MC, Gottesman MM, Maurizi MR (1993) A human mitochondrial ATP-dependent protease that is highly homologous to bacterial Lon protease. *Proc Natl Acad Sci USA* 90:11247–11251.
- Gottesman S (2003) Proteolysis in bacterial regulatory circuits. *Annu Rev Cell Dev Biol* 19:565–587.
- Bissonnette SA, Rivera-Rivera I, Sauer RT, Baker TA (2010) The IbpA and IbpB small heat-shock proteins are substrates of the AAA+ Lon protease. *Mol Microbiol* 75:1539–1549.
- Ishii Y, Sonezaki S, Iwasaki Y, Miyata Y, Akita K, Kato Y, Amano F (2000) Regulatory role of C-terminal residues of Sula in its degradation by Lon protease in *Escherichia coli*. *J Biochem* 127:837–844.
- Neher SB, Villen J, Oakes EC, Bakalarski CE, Sauer RT, Gygi SP, Baker TA (2006) Proteomic profiling of ClpXP substrates after DNA damage reveals extensive instability within SOS regulon. *Mol Cell* 22:193–204.
- Bota DA, Van Remmen H, Davies KJ (2002) Modulation of Lon protease activity and aconitase turnover during aging and oxidative stress. *FEBS Lett* 532:103–106.
- Bernstein SH, Venkatesh S, Li M, Lee J, Lu B, Hilchey SP, Morse KM, Metcalfe HM, Skalska J, Andreeff M, Brookes PS, Suzuki CK (2012) The mitochondrial ATP-dependent Lon protease: a novel target

in lymphoma death mediated by the synthetic triterpenoid CDDO and its derivatives. *Blood* 119:3321–3329.

- Liu Y, Lan L, Huang K, Wang R, Xu C, Shi Y, Wu X, Wu Z, Zhang J, Chen L, Wang L, Yu X, Zhu H, Lu B (2014) Inhibition of Lon blocks cell proliferation, enhances chemosensitivity by promoting apoptosis and decreases cellular bioenergetics of bladder cancer: potential roles of Lon as a prognostic marker and therapeutic target in bladder cancer. *Oncotarget* 5:11209–11224.
- Sauer RT, Baker TA (2011) AAA+ proteases: ATP-fueled machines of protein destruction. *Annu Rev Biochem* 80:587–612.
- Gur E, Vishkautzan M, Sauer RT (2012) Protein unfolding and degradation by the AAA+ Lon protease. *Protein Sci* 21:268–278.
- Gur E, Sauer RT (2008) Recognition of misfolded proteins by Lon, a AAA(+) protease. *Genes Dev* 22:2267–2277.
- Shah IM, Wolf RE Jr (2006) Sequence requirements for Lon-dependent degradation of the *Escherichia coli* transcription activator SoxS: identification of the SoxS residues critical to proteolysis and specific inhibition of in vitro degradation by a peptide comprised of the N-terminal 21 amino acid residues. *J Mol Biol* 357:718–731.
- Roudiak SG, Shrader TE (1998) Functional role of the N-terminal region of the Lon protease from *Mycobacterium smegmatis*. *Biochemistry* 37:11255–11263.
- Ebel W, Skinner MM, Dierksen KP, Scott JM, Trempy JE (1999) A conserved domain in *Escherichia coli* Lon protease is involved in substrate discriminator activity. *J Bacteriol* 181:2236–2243.
- Iyer LM, Leipe DD, Koonin EV, Aravind L (2004) Evolutionary history and higher order classification of AAA+ ATPases. *J Struct Biol* 146:11–31.
- Wohlever ML, Baker TA, Sauer RT (2013) A mutation in the N domain of *Escherichia coli* Lon stabilizes dodecamers and selectively alters degradation of model substrates. *J Bacteriol* 195:5622–5628.
- Wohlever ML, Baker TA, Sauer RT (2014) Roles of the N domain of the AAA+ Lon protease in substrate recognition, allosteric regulation and chaperone activity. *Mol Microbiol* 91:66–78.
- Cheng I, Mikita N, Fishovitz J, Frase H, Wintrode P, Lee I (2012) Identification of a region in the N-terminus of *Escherichia coli* Lon that affects ATPase, substrate translocation and proteolytic activity. *J Mol Biol* 418:208–225.
- Vieux EF, Wohlever ML, Chen JZ, Sauer RT, Baker TA (2013) Distinct quaternary structures of the AAA+ Lon protease control substrate degradation. *Proc Natl Acad Sci USA* 110:E2002–E2008.
- Chung CH, Goldberg AL (1982) DNA stimulates ATP-dependent proteolysis and protein-dependent ATPase activity of protease La from *Escherichia coli*. *Proc Natl Acad Sci USA* 79:795–799.
- Kuroda A, Nomura K, Ohtomo R, Kato J, Ikeda T, Takiguchi N, Ohtake H, Kornberg A (2001) Role of inorganic polyphosphate in promoting ribosomal protein degradation by the Lon protease in *E. coli*. *Science* 293:705–708.
- Mukherjee S, Bree AC, Liu J, Patrick JE, Chien P, Kearns DB (2015) Adaptor-mediated Lon proteolysis restricts *Bacillus subtilis* hyperflagellation. *Proc Natl Acad Sci USA* 112:250–255.
- Lu B, Liu T, Crosby JA, Thomas-Wohlever J, Lee I, Suzuki CK (2003) The ATP-dependent Lon protease of *Mus musculus* is a DNA-binding protein that is functionally conserved between yeast and mammals. *Gene* 306:45–55.

25. Li M, Gustchina A, Rasulova FS, Melnikov EE, Maurizi MR, Rotanova TV, Dauter Z, Wlodawer A (2010) Structure of the N-terminal fragment of *Escherichia coli* Lon protease. *Acta Cryst D* 66:865–873.
26. Delorenzi M, Speed T (2002) An HMM model for coiled-coil domains and a comparison with PSSM-based predictions. *Bioinformatics* 18:617–625.
27. Grigoryan G, Keating AE (2008) Structural specificity in coiled-coil interactions. *Curr Opin Struct Biol* 18:477–483.
28. Gur E, Sauer RT (2009) Degrons in protein substrates program the speed and operating efficiency of the AAA+ Lon proteolytic machine. *Proc Natl Acad Sci USA* 106:18503–18508.
29. Allen SP, Polazzi JO, Gierse JK, Easton AM (1992) Two novel heat shock genes encoding proteins produced in response to heterologous protein expression in *Escherichia coli*. *J Bacteriol* 174:6938–6947.
30. Laskowska E, Wawrzynow A, Taylor A (1996) IbpA and IbpB, the new heat-shock proteins, bind to endogenous *Escherichia coli* proteins aggregated intracellularly by heat shock. *Biochimie* 78:117–122.
31. Arrigo AP, Suhan JP, Welch WJ (1988) Dynamic changes in the structure and intracellular locale of the mammalian low-molecular-weight heat shock protein. *Mol Cell Biol* 8:5059–5071.
32. Bentley NJ, Fitch IT, Tuite MF (1992) The small heat-shock protein Hsp26 of *Saccharomyces cerevisiae* assembles into a high molecular weight aggregate. *Yeast* 8:95–106.
33. Torres-Cabassa AS, Gottesman S (1987) Capsule synthesis in *Escherichia coli* K-12 is regulated by proteolysis. *J Bacteriol* 169:981–989.
34. Duman RE, Lowe J (2010) Crystal structures of *Bacillus subtilis* Lon protease. *J Mol Biol* 401:653–670.
35. Lupas A (1996) Coiled coils: new structures and new functions. *Trends Biochem Sci* 21:375–382.
36. Lee AY, Hsu CH, Wu SH (2004) Functional domains of *Brevibacillus thermoruber* Lon protease for oligomerization and DNA binding: role of N-terminal and sensor and substrate discrimination domains. *J Biol Chem* 279:34903–34912.
37. Djuranovic S, Hartmann MD, Habeck M, Ursinus A, Zwickl P, Martin J, Lupas AN, Zeth K (2009) Structure and activity of the N-terminal substrate recognition domains in proteasomal ATPases. *Mol Cell* 34:580–590.
38. Carroni M, Kummer E, Oguchi Y, Wendler P, Clare DK, Sinning I, Kopp J, Mogk A, Bukau B, Saibil HR (2014) Head-to-tail interactions of the coiled-coil domains regulate ClpB activity and cooperation with Hsp70 in protein disaggregation. *Elife* 3:e02481.
39. Oguchi Y, Kummer E, Seyffer F, Berynskyy M, Anstett B, Zahn R, Wade RC, Mogk A, Bukau B (2012) A tightly regulated molecular toggle controls AAA+ disaggregase. *Nat Struct Mol Biol* 19:1338–1346.
40. Seyffer F, Kummer E, Oguchi Y, Winkler J, Kumar M, Zahn R, Sourjik V, Bukau B, Mogk A (2012) Hsp70 proteins bind Hsp100 regulatory M domains to activate AAA+ disaggregase at aggregate surfaces. *Nat Struct Mol Biol* 19:1347–1355.
41. Carroni M, Franke KB, Maurer M, Jager J, Hantke I, Gloge F, Linder D, Gremer S, Turgay K, Bukau B, Mogk A (2017) Regulatory coiled-coil domains promote head-to-head assemblies of AAA+ chaperones essential for tunable activity control. *Elife* 6:e30120.
42. Shearstone JR, Baneyx F (1999) Biochemical characterization of the small heat shock protein IbpB from *Escherichia coli*. *J Biol Chem* 274:9937–9945.
43. Schuck P (2000) Size-distribution analysis of macromolecules by sedimentation velocity ultracentrifugation and lamm equation modeling. *Biophys J* 78:1606–1619.
44. Lindsley JE (2001) Use of a real-time, coupled assay to measure the ATPase activity of DNA topoisomerase II. *Methods Mol Biol* 95:57–64.
45. Gottesman S, Roche E, Zhou Y, Sauer RT (1998) The ClpXP and ClpAP proteases degrade proteins with carboxy-terminal peptide tails added by the SsrA-tagging system. *Genes Dev* 12:1338–1347.